Monolithically Integrated High-Q Rings for Narrow Linewidth Widely Tunable Lasers

Tin Komljenovic and John E. Bowers, *Fellow, IEEE*

(Invited Paper)

***Abstract*— We theoretically analyze the use of fully integrated high-Q ring cavities (intrinsic $Q \sim 1$ million) with widely tunable semiconductor lasers to realize narrow linewidth lasers. Different configurations are studied, including cases where the high-Q cavity is external to the laser cavity and provides filtered optical feedback to the laser cavity and cases where the high-Q cavity is an integral part of the laser cavity. We show that the current heterogeneous silicon platform should allow subkilohertz instantaneous linewidths, and we outline the advantages and disadvantages of different high-Q cavity placements.**

***Index Terms*— Semiconductor lasers, cavity resonators, laser tuning, photonic integrated circuits.**

I. Introduction

WIDELY-TUNABLE monolithically integrated lasers (WTMIL) have been attracting great interest [1], [2], as they are a perfect candidate for dense wavelength division multiplexing (DWDM) communication systems and for a variety of optical sensing applications and systems. Communication systems have recently moved to more complex modulation formats that require higher spectral purity lasers [3], so narrow-linewidth, together with wide-tunability, have became a focus of research [4], [5]. WTMILs offer size, weight and cost advantages compared to mechanically tuned external-cavity lasers, but typically have higher phase noise limiting the applicability in coherent communication systems, and feature mode-hops limiting the applicability in certain sensing applications. Linewidths of III-V semiconductor lasers have typically been in the few MHz range, and recently sub-MHz instantaneous linewidths have been demonstrated [6]. The main restriction in further improvement of linewidth with III-V designs comes from the limitation in obtainable Q factor of the resonator, as photon generation and storage are made in the same material. Heterogeneous silicon photonics removes this limitation by combining the efficient III-V electrically-pumped sources and low-loss silicon waveguides. The ability to make high-Q photon storage in silicon allowed integrated linewidths as low as 50 kHz for widely-tunable lasers [5] and sub-kHz instantaneous linewidths for single-frequency lasers [7]. Both are fully monolithically-integrated designs. In this paper we explore a possibility of improving the linewidth of WTMILs by utilizing an integrated high-Q ring cavity-on-chip. We analyze three potential strategies: with the high-Q ring used as an external cavity with optical feedback in all-pass or drop configurations, and with the high-Q ring being an integral part of the laser cavity. The paper is organized as follows. In Section II we give a brief overview of WTMIL designs utilizing rings and analyze the most common architecture in terms of linewidth performance. To this end we utilize the theory of adiabatic chirp reduction. In Section III we introduce external high-Q ring cavity, modify the negative optical feedback theory and apply it to two representative external ring cavity configurations. We turn to narrow-linewidth enabled by using high-Q ring cavities in Section IV. We analyze all three outlined strategies for narrow-linewidth and provide linewidth estimates and other relevant characteristics of such laser architectures. Finally we summarize, give conclusions, and present a table outlining advantages and disadvantages of specific approaches in Section V.

Manuscript received July 29, 2015; revised September 13, 2015; accepted September 16, 2015. Date of publication September 22, 2015; date of current version October 19, 2015. This work was supported in part by the Defense Advanced Research Projects Agency under Contract EPHI and Contract DODOS. The work of T. Komljenovic was supported by NEWFELPRO under Grant 25.

The authors are with the University of California at Santa Barbara, Santa Barbara, CA 93106 USA (e-mail: tkomljenovic@ece.ucsb.edu; bowers@ece.ucsb.edu).

Color versions of one or more of the figures in this paper are available online at http://ieeexplore.ieee.org.

Digital Object Identifier 10.1109/JQE.2015.2480337

II. Widely-Tunable Ring Based Lasers

Wide-tunability in semiconductor lasers is commonly achieved by utilizing the Vernier effect. The effect has been utilized both with sampled Bragg grating reflectors and ring resonators. Ring resonators, provided that the utilized waveguide platform offers sufficiently low propagation losses, have an advantage as the effective cavity length at ring resonance is significantly enhanced, directly influencing linewidth [8], [9]. For this reason we concentrate on ring-based lasers.

Many ring-based laser topologies have been studied (see Fig. 1). The Vernier-based ring laser [10] features a ring-based cavity topology and allows for clockwise (CW) and counterclockwise (CCW) propagating modes. The output power at the single output port is somewhat compromised by allowing CW and CCW propagating modes and including unwanted ports through which useful laser light is left untapped. The number of output ports can be reduced by utilizing the coupled ring resonator (CRR) approach [11] where a pair of identical rings is used to realize a frequency-dependent reflector. An advantage of using a CRR mirror design is that it avoids having a drop port bus waveguide to form the necessary filter shape and results with a simple two output-port laser. Tuning of such structures is more challenging as the radii of the rings comprising a CRR have to be

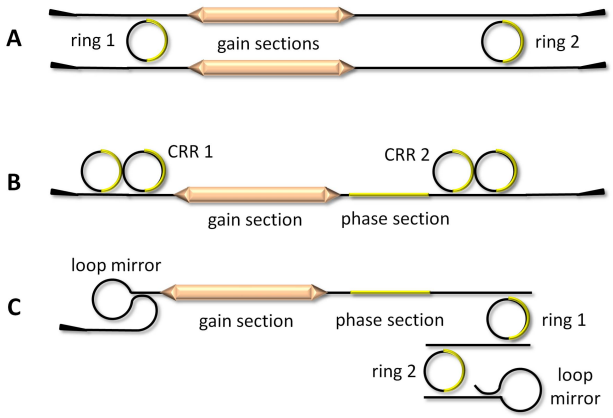

Fig. 1. Common widely-tunable ring based laser designs. (A) Vernier ring laser [10] (B) Coupled ring resonator (CRR) based laser [11] (C) Single-wavelength ring filter based laser [4], [5], [12]. Gain sections are orange, yellow shows tuning elements – most commonly realized as heaters.

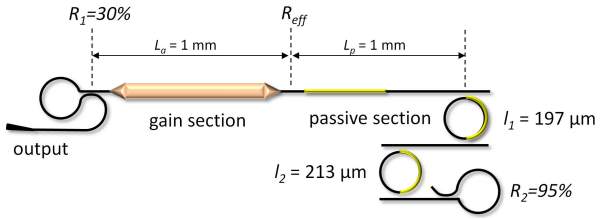

Fig. 2. Schematic of widely-tunable single-wavelength laser with dimensions of cavity elements. The power coupling coefficient (κ^2) between rings and bus waveguides is equal to 15% in all cases.

identical, often to a degree surpassing typical semiconductor process tolerances. Additionally, the degeneracy of identical rings can result in mode-splitting in reflected spectra. For proper operation, all four rings have to be independently controlled, complicating the operation of such a laser. A third approach uses a single-wavelength filter (SWF) at one side of the cavity, most commonly formed by two loop-mirrors. The SWF is usually placed at the back of the cavity in order to maximize the differential quantum efficiency at the output port. This configuration allows easy control of the output direction by adjusting the loop mirror reflectivities, and simplifies the tuning with only two rings with slightly different radii. This design is most commonly used today to realize wide-tuneability [4], [5], [12] and it is the one we will use for this theoretical study of linewidth narrowing by using a high-Q ring cavity.

A. Laser Parameters

In our analysis, we assume a laser operating at 1550 nm, with a 1 mm long gain section (L_a) and a 1 mm long passive section (L_p) as shown in Fig. 2. The passive section includes all of the delay inside the cavity from waveguides to loop mirrors, waveguides between the ring resonators, etc. We identify two reference planes R_1 and R_{eff}. R_1 is the power reflectivity of the output mirror, assumed to be 30%, while R_{eff} is the effective power reflectivity of the combination of the SWF (comprised of two ring resonators), the loop mirror, and the delay due to passive section. We use capital R for power reflectivities and small r for amplitude reflectivities throughout this manuscript, where $R = |r|^2$. We use the same R_{eff} plane for all of the calculations, so R_1 and R_{eff} form an equivalent optical cavity where the effective mirror has a complex wavelength dependence of its amplitude reflectivity. This substitution is valid for steady-state analysis [13]. The radii of tuning rings are not critically important for our analysis, and should be adjusted to provide wide-tuning and single-wavelength operation. We set the circumference of ring 1 to be $l_1 = 197$ μm and the circumference of ring 2 to be $l_2 = 213$ μm. We assume an effective index of refraction to be uniform in all sections of the laser, for simplicity, and set it at $n_{eff} = 3.8$. We neglect the wavelength dependence of the effective index of refraction, again for simplicity. For this given effective index of refraction, the free spectral ranges (FSRs) of our rings are 370 GHz and 400 GHz, or 2.97 nm and 3.21 nm. The wavelength tuning enhancement factor [9] due to the Vernier effect, $M = l_1/(l_2 - l_1)$, is equal to 12.31 resulting in ~39.5 nm of tuning range. We assume 15% power coupling (κ^2) in the SWF rings at all coupling interfaces and neglect coupling loss. The propagation loss is assumed to be 0.5 dB/cm in all passive segments of the laser [4]. The complex amplitude reflectivity r_{eff} is given by the following expressions:

$$r_{eff} = (S_{21,passive})^2 \cdot (S_{21,ring1})^2 \cdot (S_{21,ring2})^2 \cdot r_2, \tag{1}$$

$$S_{21,passive} = e^{-\alpha_p L_p} e^{-j\beta_p L_p}, \tag{2}$$

$$S_{21,ringX} = \frac{|\kappa|^2 X_X}{1 - \tau^2 X_X^2}, \tag{3}$$

$$X_x = e^{-\alpha_p \frac{l_X}{2}} e^{-j\beta_p \frac{l_X}{2}}. \tag{4}$$

where α_p, and β_p are the waveguide electric field propagation loss and the effective propagation constant in waveguides respectively, r_2 is the amplitude reflectivity of the back-side mirror, l_X is the length (circumference) of the ring, and the subscript X takes values 1 and 2 for the two rings in the SWF section.

To analyze the linewidth, we turn to the theory of adiabatic chirp reduction and narrowing of the Lorentzian laser linewidth due to coupling of the laser to an external passive resonator [14]. The coupling is expressed via complex, wavelength dependent mirror reflectivity (r_{eff}). The chirp reduction is described by a factor $F = 1 + A + B$ and the Lorentzian linewidth ($\Delta\nu_0$) is reduced by F^2.

$$\Delta\nu = \frac{\Delta\nu_0}{F^2} \tag{5}$$

$$A = \frac{1}{\tau_{in}} \mathrm{Re}\left\{ i \frac{d}{d\omega} \ln r_{eff}(\omega) \right\} = -\frac{1}{\tau_{in}} \frac{d\varphi_{eff}(\omega)}{d\omega} \tag{6}$$

$$B = \frac{\alpha_H}{\tau_{in}} \mathrm{Im}\left\{ i \frac{d}{d\omega} \ln r_{eff}(\omega) \right\} = \frac{\alpha_H}{\tau_{in}} \frac{d}{d\omega} \left(\ln(|r_{eff}(\omega)|) \right) \tag{7}$$

where α_H is the linewidth enhancement factor assumed to be equal to 4 throughout the analysis. $\tau_{in} = 2n_{eff}L_a/c$ where n_{eff} is the effective index of the gain section assumed to be 3.8, and c is the speed of light. For our considered case,

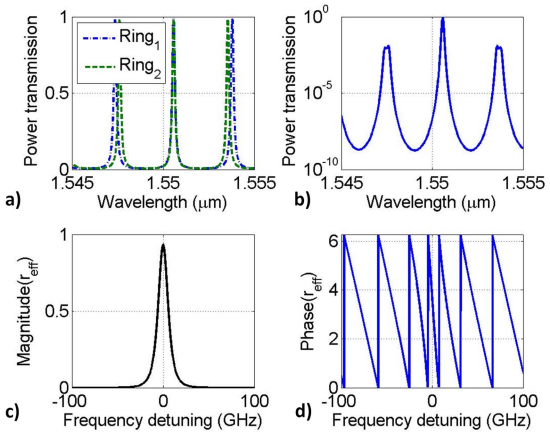

Fig. 3. (a) Drop-port transmissions of two rings forming the widely-tunable single-wavelength filter (SWF) (b) The power transmission of the passive section of the laser and the Vernier effect due to rings of slightly different radii (c) Magnitude of complex amplitude reflectivity r_{eff} (d) Phase of the complex amplitude reflectivity r_{eff}.

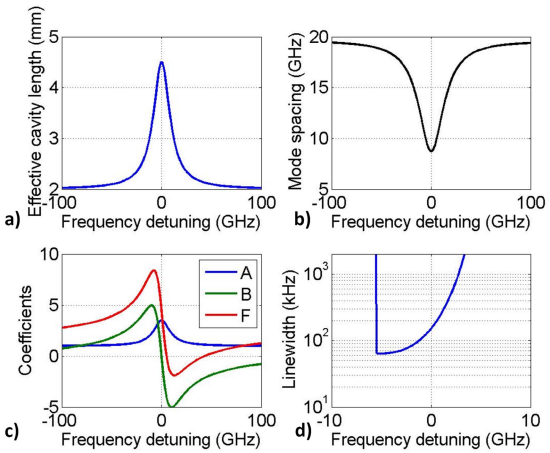

Fig. 4. (a) Effective cavity length (b) Longitudinal mode spacing (c) Coefficients A, B and F calculated from (5), (6) and (7) (d) Theoretically estimated instantaneous linewidth; all as a function of detuning from SWF resonance.

$\tau_{in} \approx 25.3$ ps. We assume a loss $\alpha_a = 20$ cm^{-1} in the active section, intentionally selecting a high value as a worst case. The A term, corresponding to the linewidth reduction from reduced longitudinal mode confinement, is often denoted as the ratio of the external (passive section) cavity path length to the gain section path length. As the effective length of a ring resonator is maximized at resonance, the A factor is maximized when the ring is placed exactly at resonance. The B term corresponds to the reduction from the negative feedback effect where a decrease in wavelength increases reflectivity (increasing photon density in the cavity) and hence decreases carrier density, which in turn causes the wavelength to increase due to the carrier plasma effect. The phase condition in the cavity can be used for a slight detuning of the laser oscillation with respect to the minimum cavity loss condition (resonator resonance). Figs. 3 and 4 show simulations for the widely-tunable single-wavelength laser. Due to cavity length enhancement of rings at resonance, the longitudinal mode spacing is reduced from 20 GHz to 8.75 GHz. The linewidth due to the feedback from the effective mirror can theoretically be reduced by $\sim 55\times(F = 7.41)$ with lowering the lasing frequency with respect to ring resonance. The model used in plot Fig. 4.d takes into account the widening of active-section effective-cavity Schawlow-Townes linewidth due to the reduced effective back-mirror reflection, i.e. increased cavity loss, with detuning. As a result, the optimal linewidth position is not at the maximum F value, but is still on the lower frequency side of the ring resonance. For the considered lasers, $\sim$60 kHz instantaneous linewidths should be obtainable at 3 dBm output powers.

III. External High-Q Ring Cavity

We first study the ability of the high-Q ring cavity to provide external optical feedback. External optical feedback has been shown to be an effective technique to modify intrinsic semiconductor laser properties [15] and has been extensively studied in configurations where the external cavity is not monolithically integrated with the laser [16], [17]. The laser performance can be influenced by coupling the laser to a distanced single mirror or to a high-Q cavity. We have analyzed, designed and measured the performance of a WTMIL coupled to an external mirror [5] and have shown that the external cavity, formed between the external mirror and one facet of the laser, can reduce the integrated linewidth to 50 kHz and that further improvements are possible. For a laser coupled to a single mirror, two modes of operation can be identified, depending on if the external cavity free-spectral range is larger or smaller than the relaxation oscillation frequency (ω_R) of the standalone laser [15]. For short cavities (external cavity FSR $> \omega_R$), the linewidth reduction is modest, but the feedback system has a very broad effective bandwidth able to suppress noise to frequencies much larger than ω_R. In the case of a long cavity (external cavity FSR $< \omega_R$), the linewidth reduction can theoretically be much greater, but the effective bandwidth of the feedback system is narrower, resulting in strong external cavity modes. For stronger feedback, external cavity modes grow and can cause the laser to become unstable. The optimal choice for narrow linewidth would therefore be an external cavity slightly shorter (FSR slightly larger) than ω_R with relatively strong feedback.

The limitation can be circumvented by coupling to a separate external cavity instead of a mirror. This has been typically done with Fabry-Perot cavities that were free-space coupled to semiconductor lasers [16], [17]. The use of a separate cavity for feedback breaks the limitation as one can engineer the cavity to have the FSR larger than ω_R, keeping the laser stable with large effective bandwidth and offering narrow linewidth due to increased photon lifetime inside the cavity [15]. One of the benefits of integration is the reduced coupling loss between the laser and the external cavity.

For an integrated design, one can use a ring resonator as an external cavity utilizing the lower propagation loss provided by a silicon (or silicon nitride) waveguide. The propagation loss is assumed to be 0.5 dB/cm [4] resulting in internal Q in the range of 1.4 million. The coupling can be optimized for particular high-Q ring placement as shown in Section IV.

We analyze the external cavity configurations in two ways. We study the frequency chirp reduction due to the external cavity using the effective reflectivity approach as outlined in Section II.A and we show the results of this analysis in Section IV. Here we study the bandwidth of the negative optical feedback following the procedure outlined in [18]. We modify the analysis to the spectral domain as it simplifies the calculations with ring resonators and compound cavities in general.

A. Bandwidth Analysis of Negative Optical Feedback

To calculate the response of the cavity (namely responsivity and phase delay) when light with a finite linewidth due to phase/frequency noise fluctuations is incident, we approximate the finite linewidth with frequency modulated light:

$$v(t) = v_0 + v_m \cos(2\pi f_m t) \tag{8}$$

where v_0 is the optical frequency of non-modulated light, f_m is the modulation frequency and v_m is the maximum optical frequency excursion of the light [16], [18]. The incident optical field in the time-domain can be written as:

$$E_{in}(t) = E_0 \exp\left[j\left(2\pi v_0 t + \frac{v_m}{f_m}\sin(2\pi f_m t)\right)\right]. \tag{9}$$

Setting $\Omega = 2\pi v_0$ and $\beta = v_m/f_m$ we arrive to a simpler expression and transform it to the frequency domain:

$$\begin{aligned} E_{in}(t) &= E_0\left[\sum_{n=-\infty}^{\infty} J_n(\beta)\cos((\Omega + n w_m)t)\right] \\ \Rightarrow\ E_{in}(f) &= E_0 \sum_{n=-\infty}^{\infty} J_n(\beta)\delta(f-(v_0+nf_m)) \end{aligned} \tag{10}$$

where J_n is the Bessel function of the first kind and n-th order. The reflected field can now easily be computed by calculating the S_{11} parameter of the whole external cavity.

$$\begin{aligned} E_{out}(f) &= E_0 \sum_{n=-\infty}^{\infty} J_n(\beta)\cdot S_{11}\,(v_0+nf_m)\,\delta(f-(v_0+nf_m)) \\ \Rightarrow E_{out}(t) &= \mathrm{Re}\left\{ E_0 \sum_{n=-\infty}^{\infty} J_n(\beta)\cdot S_{11}\,(v_0+nf_m) \right. \\ &\qquad \left. \times e^{j2\pi(v_0+nf_m)t}\right\} \end{aligned} \tag{11}$$

Neglecting the oscillations at the optical frequency, we fit the response of the cavity to

$$R(t) = R_0 + \Delta R(f_m)\cdot\cos\{2\pi f_m t + \varphi(f_m)\} \tag{12}$$

where $\Delta R(f_m)$ and $\varphi(f_m)$ are fitting parameters as a function of f_m. We define the transfer function of resonator H_{res} and transfer function of the delay loop H_{loop} as:

$$H_{res} = \frac{\Delta R(f_m)}{v_m}\exp(-j\varphi(f_m)) \tag{13}$$

$$H_{loop} = \exp\left(-j2\pi f_m \tau_{loop}\right), \quad \tau_{loop} = \frac{2n_{eff}L_{loop}}{c} \tag{14}$$

where L_{loop} is the distance between the laser and the resonator (see Fig. 5). For the negative optical feedback to be stable there should be no phase inversion in the region with positive gain. The region with positive gain is most easily approximated with the relaxation oscillation frequency of the laser as laser response drops rapidly beyond that point. For the laser architecture commonly used and described in detail in Section II, relaxation oscillation frequency was measured to be in the range of 2 GHz [5]. The phase delay arises due to the resonator response and due to the delay between the laser and the resonator, so the negative optical feedback system can be resonator- or delay-limited. Reducing the delay is always beneficial and is one of the strengths of using a fully integrated approach. On the other hand, the responsivity should be maximized in the region where the system is stable to maximize the effect of negative optical feedback. We consider two configurations as shown in Fig. 5. The drop ring resonator configuration has two coupling points. Minimum insertion loss (or maximum power transfer to the drop channel) occurs at asymmetric coupling where the input is set at critical coupling condition with regard to the internal loss and drop port coupling. Regardless, symmetric coupling has commonly been utilized [19] and we use the same approach here – equating the two coupling values. The approach is further justified, as we use the resonator in both directions (two-pass configuration) making the asymmetric coupling optimization for lowest insertion loss unfeasible. We show simulation results of responsivity in Fig. 6. We show results for three ring lengths of 1.25 mm, 3.14 mm and 5.02 mm, corresponding to radii of 200 μm, 500 μm and 800 μm. For the all-pass configuration (full lines), responsivity is maximized at slight under-coupling, while for the drop resonator configuration (dashed lines) there is an optimal coupling point dependent on ring circumference (and round-trip loss). For the considered drop configuration cases, the responsivity is maximized at relatively high power coupling values. In a first order approximation, for low ring roundtrip losses, one can use any ring length for a given propagation loss and have the same loaded Q when the resonator is critically coupled. In practice, for low propagation loss a less confined waveguide geometry is needed, limiting the bend radius. Therefore larger radii rings will provide better performance.

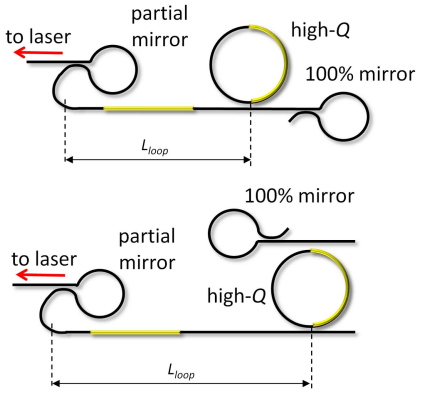

Fig. 5. Two considered external high-Q cavity configurations. (Up) Ring resonator in all-pass configuration (Down) Ring resonator in drop configuration.

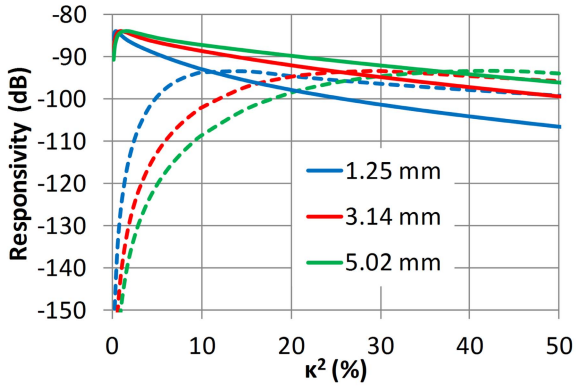

Fig. 6. Responsivity or magnitude of H_{res} in (13) for various coupling coefficients at low-frequency (10 MHz). (*Full line*) All-pass resonator configuration (*Dashed line*) Drop resonator configuration. Different colors correspond to different ring resonator circumferences (0.5 dB/cm propagation loss).

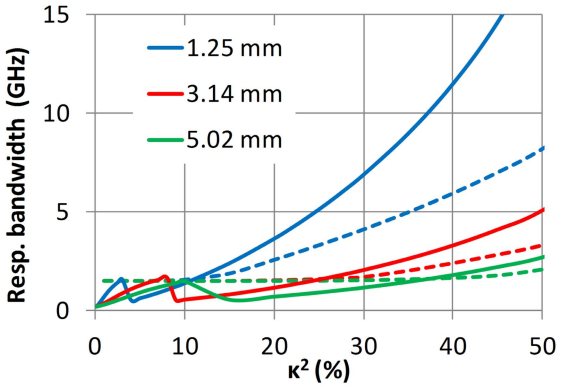

Fig. 7. Responsivity bandwidth defined as frequency where responsivity (Fig. 6) falls by 3 dB. (*Full line*) All-pass resonator configuration (*Dashed line*) Drop resonator configuration. (0.5 dB/cm propagation loss).

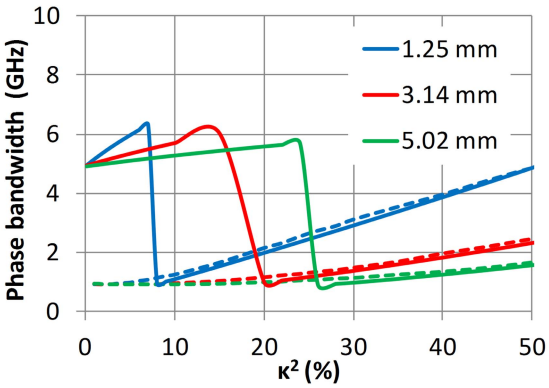

Fig. 8. Phase bandwidth defined for phase margin of 45°. The plot shows frequency where phase surpasses 135° shift, potentially leading to positive feedback and detrimental laser performance. (*Full line*) All-pass resonator configuration (*Dashed line*) Drop resonator configuration. At higher coupling strengths in all-pass configuration the phase response changes dramatically (see Fig. 9) and approaches that of drop configuration. (0.5 dB/cm propagation loss, 1 mm loop delay).

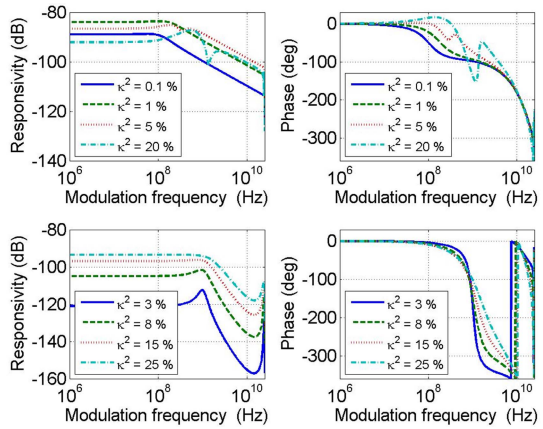

Fig. 9. Some exemplary responsivity and phase traces. (Up) All-pass resonator configuration, (Down) drop resonator configuration for various coupling coefficients ($r = 500$ μm, 0.5 dB/cm propagation loss, 1 mm delay).

There are two bandwidths of interest in negative optical feedback. First is the 3 dB bandwidth of responsivity, shown in Fig. 7. Although the apparent bandwidth of the all-pass configuration is generally smaller than the drop configuration for a range of coupling values, low-frequency responsivity is typically 10 dB higher at optimal coupling and the roll-off is 10 dB/decade (see Fig. 9), so better performance is typically expected with a properly coupled all-pass ring resonator configuration. The second bandwidth parameter is related to the phase of the returned signal and is the most important parameter for proper operation of the negative optical feedback. Under excessive delay, negative feedback can become positive. We define phase bandwidth as the frequency where the phase equals $-135°$, providing a phase margin of 45° similar to electrical feedback loops [20]. We show simulated results in Fig. 8 assuming a 1 mm loop delay (L_{loop}). The phase bandwidth of the drop configuration steadily increases as the coupling is increased, but that lowers the loaded Q of the resonator as was already pointed out. The all-pass configuration has two regions of operation. For high coupling values, performance is very similar to the performance of drop configuration, but for lower coupling strengths, the phase bandwidth is significantly improved. The cross-over point happens at a coupling strength of approximately $4\times$ the critical coupling value. Some exemplary reponsivity and phase plots are shown in Fig. 9. For the all-pass configuration, better responsivity at lower frequencies is obtained for slight undercoupling, while at higher frequencies the performance is improved with slight overcoupling. The coupling has significant influence on phase response, with a resulting notch when overcoupled, and this notch reduces the phase bandwidth at significant over-coupling as shown in Fig. 8.

IV. Narrow-Linewidth With High-Q Rings

Next, we analyze three potential strategies for obtaining narrow-linewidth utilizing high-Q rings using the theory of adiabatic chirp reduction [14]: with the high-Q ring used as an external cavity, with optical feedback in all-pass or drop configurations, and with high-Q ring being an integral part of the laser cavity. In the analysis that follows, we set the ring 3 (high-Q ring) radius to 500 μm (circumference equals 3.14 mm) resulting in a FSR of 25 GHz.

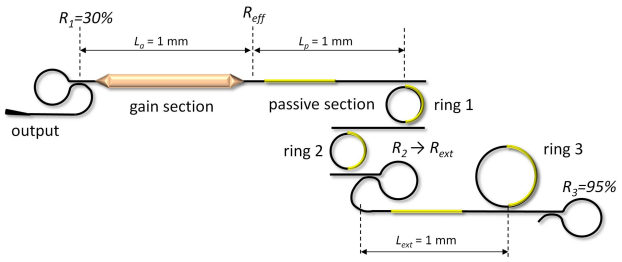

Fig. 10. Schematic of external cavity laser with high-Q ring in all-pass configuration.

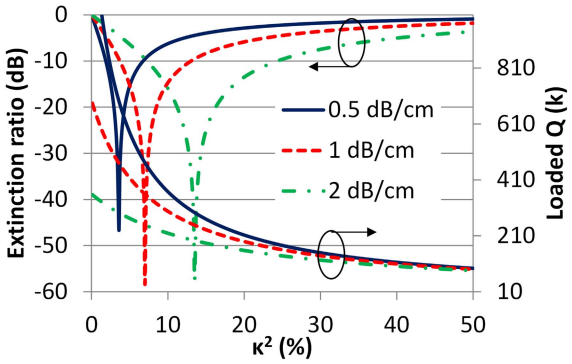

Fig. 11. Extinction ratio (single-pass) and loaded Q of ring resonator in all-pass configuration as a function of coupling strength for three propagation loss values.

A. External All-Pass High-Q Cavity Laser

The proposed laser architecture is shown in Fig. 10 and features a standard widely-tunable laser design whose back mirror is adjustable and couples the laser to an external ring resonator in an all-pass configuration and a loop mirror. The total delay in the external cavity (excluding the delay due to ring resonator) is absorbed into a variable L_{ext} and is set at 1 mm. To analyze the performance, we first transform R_2 and the external cavity to an effective mirror labeled R_{ext}. Then we transform this effective mirror R_{ext}, two rings used in the tuning section (SWF), and the laser passive section, into an effective mirror labeled R_{eff}. R_1 and R_{eff} then make a simple FP-cavity laser where one of the mirrors is complex and is a function of wavelength. The external feedback modulates the reflectivity R_2 of the laser cavity mirror and is superimposed over the Vernier filter formed by two smaller radii rings. We utilize the same approach when analyzing architectures described in Section IV.B and IV.C.

Coupling of the external high-Q ring resonator is an optimization parameter. The placement of the high-Q ring in an all-pass configuration allows for higher loaded Qs. For the all-pass configuration, the highest extinction ratio (ER) is achieved when the ring is critically coupled but the ER quickly decreases as coupling is changed from a critical one (see Fig. 11). The degradation of ER is slower in an over-coupled regime, and e.g. setting $\kappa^2 = 5\%$ for 0.5 dB/cm provides ideally ~15 dB of ER and provides tolerance due to process variation in a practical design. The loaded Q is ~580k. We can identify two regimes of operation. When the

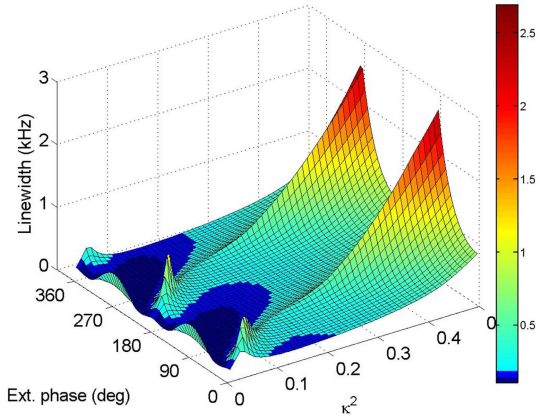

Fig. 12. Minimum linewidth for configuration shown in Fig. 10 as a function of κ^2 for ring 3 and the phase tuning of the external cavity formed between R_2 and R_3. Ring 3 is aligned with SWF. The periodicity is 180° due to signal passing twice through the phase shifter. The power reflectivity $R_2 = 0.15$. Propagation loss 0.5 dB/cm.

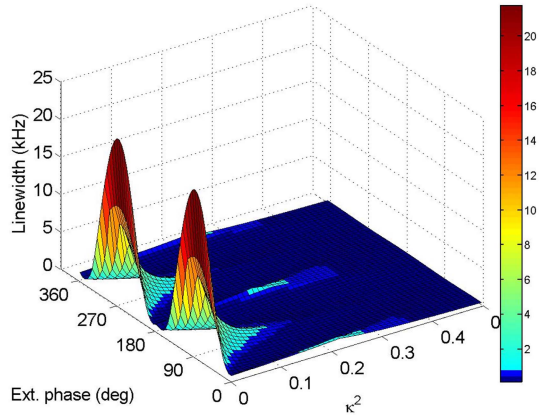

Fig. 13. Same as in Fig. 12, but with power reflectivity $R_2 = 0.85$.

reflectivity of the mirror R_2 is low, the laser effectively has a long cavity loaded with a high-Q ring and the performance is mostly dominated by the ring resonator, although it is also influenced by the phase relationship between the ring cavity and the weak FP cavity formed between R_2 and R_3. When the reflectivity of R_2 is high, the laser has a shorter cavity where the laser cavity mirror R_2 is frequency modulated by the feedback provided both by the high-Q ring and the FP cavity formed between R_2 and R_3. For a 1 mm delay, the FSR of this additional FP cavity is ~40 GHz and the complex interaction between the two cavities allows for a narrow-linewidth in a wide range of ring 3 coupling values. In Figs. 12 and 13, we plot the minimum linewidth obtainable by detuning the laser operating frequency by up to 5 GHz from R_{eff} peak value and utilizing negative optical feedback for narrow linewidth as a function of ring 3 coupling and phase of the external cavity. By controlling the phase condition inside the cavities and placing the lasing frequency at optimum position, sub-kHz instantaneous linewidths should readily be obtainable (dark blue colored regions shown in Figs. 12 and 13). We set the minimum R_{eff} value in the optimization routine to 30%.

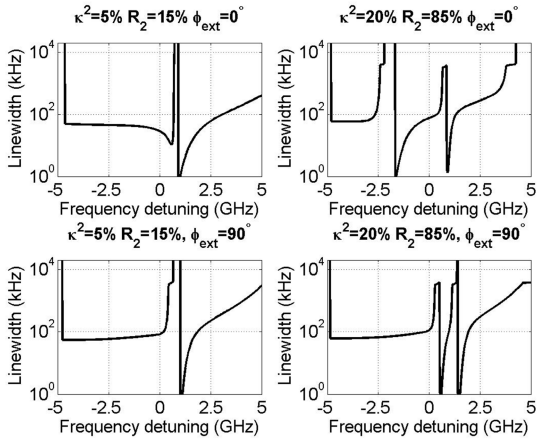

Fig. 14. Theoretical instantaneous linewidth vs. laser operating frequency detuning from R_{eff} maximum value. Coupling, R_2 reflectivity and phase of external FP cavity are plotted above each subfigure. Sub-kHz instantaneous linewidths should be obtainable, but the operation is complicated due to extreme sensitivity of linewidth on laser operating frequency.

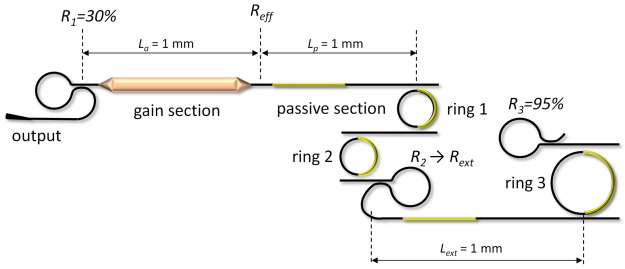

Fig. 15. Schematic of external cavity laser with high-Q ring in drop configuration.

Typical detuning from minimum loss is on the order of 1 GHz and introduces ∼4 dB of loss. The issue is that regions of stability are narrow and linewidths tends to degrade as the laser is operated on the other slope of resonance (see Fig. 14), so control of such a laser is very challenging – bandwidths (defined as frequency range where linewidth stays $<2x$ of narrowest linewidth) are in ∼50 MHz range. Furthermore, phase adjustment of all cavities is necessary for good performance. Another possible issue is the filtering of a single longitudinal mode of such a laser structure. Due to significant cavity length enhancement under certain operating conditions, the longitudinal mode spacing can be reduced to sub-GHz values which are difficult to filter with the proposed SWF configuration so laser can become unstable under stronger feedback (lower R_2 values).

B. External Drop High-Q Cavity Laser

The proposed laser architecture is shown in Fig. 15. The total delay in the external cavity (excluding the delay due to ring resonator) is again absorbed into a variable L_{ext} and is set at 1 mm. In this configuration, ring 3 acts as a filter for feedback signal, and its insertion loss (IL) should be minimized. IL can be minimized either by increasing the intrinsic Q (reducing the internal losses) or by increasing the loading (coupling value) [19]. For a given propagation loss, loading

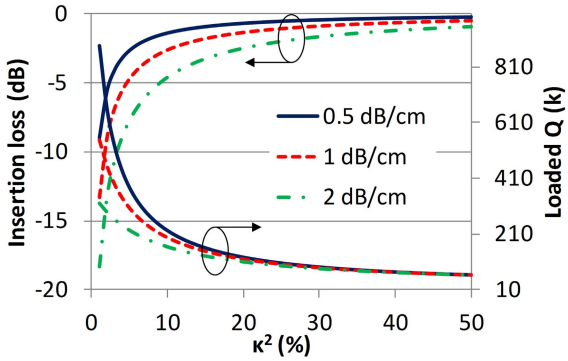

Fig. 16. Insertion loss (single-pass) and loaded Q of ring resonator in add-drop configuration as a function of coupling strength (assumed to be equal at both coupling points) for three propagation loss values.

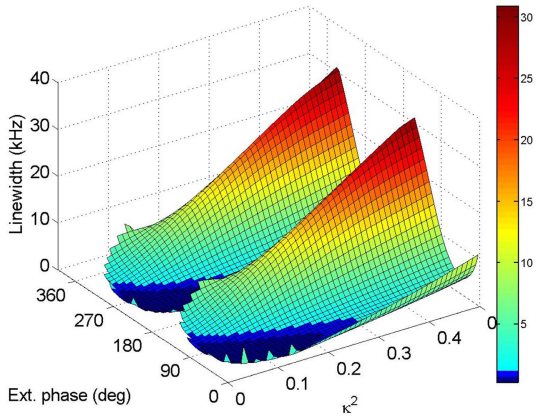

Fig. 17. Minimum linewidth for configuration shown in Fig. 15 as a function of κ^2 for ring 3 and the phase tuning of the external cavity formed between R_2 and R_3. Ring 3 is aligned with SWF. The periodicity is 180° due to signal passing twice through the phase shifter. The power reflectivity $R_2 = 0.15$. Propagation loss 0.5 dB/cm.

of the resonator is the only option to reduce IL, but it comes at the expense of a reduction of the total Q (see Fig. 16), potentially limiting the linewidth improvement due to feedback. Coupling strength (κ^2) of 15% results with 0.92 dB of single-pass IL due to ring 3. The loaded Q is ∼160k. Depending on the value of R_2 we can once again discern two characteristic regions of operation. For low values of R_2 the total reflection is low and is substantially increased at the resonant condition of the external resonator. For higher values of R_2 the reflection is high, and is predominantly reduced by external resonator. Sub-kHz instantaneous linewidths are, once again, readily obtainable (dark blue colored regions shown in Figs. 17 and 18). In the case of a lower R_2 reflection, narrow-linewidth is obtained at lower κ^2 values where Q is higher, while for higher R_2 values, narrow-linewidth is obtained in a wide range of coupling values by utilizing mode-splitting between stronger external FP cavity and ring resonator. For the best performance, alignment of all cavities is once again required. In cases where factor A (6) is large, longitudinal mode spacing reduces to GHz levels. The filtering of a single mode is facilitated somewhat by a narrower response of the whole filter subsection, where filtering improves for

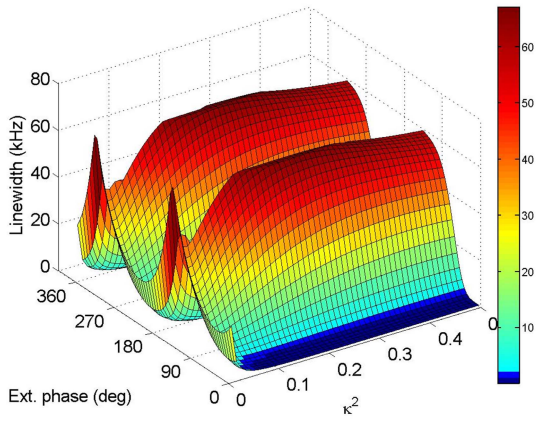

Fig. 18. Same as in Fig. 17, but with power reflectivity $R_2 = 0.85$.

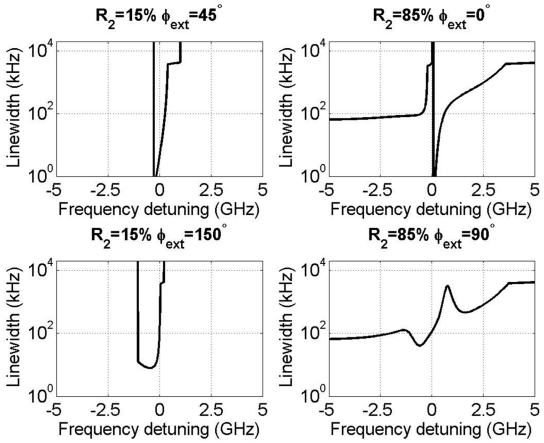

Fig. 19. Theoretical instantaneous linewidth vs. laser operating frequency calculated for $\kappa^2 = 15\%$. R_2 reflectivity and phase of external FP cavity are plotted above each subfigure. Sub-kHz instantaneous linewidths should be obtainable, but require tight control of laser operating frequency and phase alignment between cavities.

lower values of R_2. The linewidth improvement is generally lower than the all-pass configuration, but the optimal regions are a bit broader (∼100 MHz) so operation of such a laser could be less constrained by longer-term wavelength stability. As longitudinal mode filtering and linewidth both tend to improve with reduction of R_2, a natural question arises of why not design a laser with $R_2 = 0$. We study that configuration in the next section.

C. High-Q Ring as a Part of Laser Cavity

Fig. 20 shows the proposed laser architecture where the high-Q ring is in a drop-configuration as an integral part of the laser cavity. The length of the passive section (that includes all of the delay inside the laser cavity, except the delay in the gain section and inside the rings) is increased to 2 mm to include the additional waveguide length used to lay out the bus waveguides in a ring resonator structure. The inclusion of another ring resonator inside the cavity increases the cavity loss and there is a trade-off in the loaded Q and insertion loss (see Fig. 16). Dual-pass excess loss due to the inclusion of the third ring is 1.84 dB for $\kappa^2 = 15\%$, so by combining the ring 3

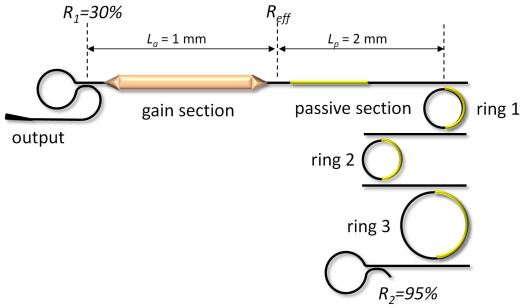

Fig. 20. Schematic of laser with high-Q ring inside the cavity.

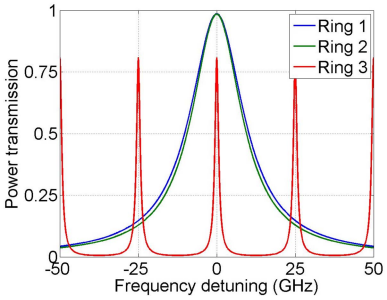

Fig. 21. Ring 1 and 2 filter-out a single resonance of ring 3 and provide for wide-tunability due to Vernier effect (plotted for $\kappa^2 = 15\%$ and propagation loss of 0.5 dB/cm).

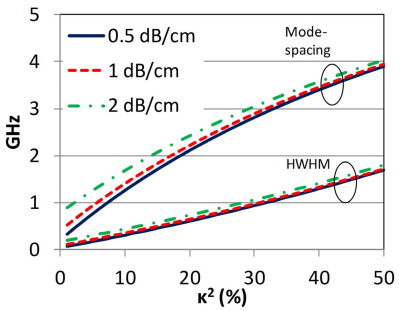

Fig. 22. Longitudinal mode spacing of laser cavity and half-width at half-maximum (HWHM) of ring 3 resonator as a function of ring 3 coupling strength. HWHM effectively shows how close neighboring longitudinal mode can be while having at least 3 dB of suppression.

with R_2 mirror, one arrives at resonance to a reflector with an effective reflectivity of ∼62%, terminating a standard widely-tunable single-wavelength laser. Qs of the tuning section rings (ring 1 and 2) are on the order of 10k, while the narrow-linewidth ring (ring 3) features a loaded Q of ∼160k for the given power coupling.

Rings 1 and 2 are used to filter out a single resonance of ring 3 whose spacing is equal to 25 GHz (see Fig. 21). Ring 3 is used to filter out a single mode of the longitudinal cavity, whose spacing is a function of the ring Q and the detuning from ring resonances. Simulation results, shown in Fig. 22, demonstrate that single-wavelength operation is straightforward to achieve. Furthermore, the phase of only one cavity has to be optimized for best performance.

The instantaneous linewidth as a function of ring 3 coupling (κ^2) and its alignment to SWF is shown in Fig. 23. Dark blue regions are the ones with ∼ kHz linewidths.

TABLE I
COMPARISON OF HIGH-Q RING INTEGRATION STRATEGIES

High-Q ring location	Advantages	Disadvantages
External (all-pass configuration)	- Potentially narrowest linewidth - Wider negative optical feedback bandwidth - Higher responsivity of negative optical feedback	- Extreme sensitivity of laser linewidth to operating frequency - Potential multimoding at higher external feedback levels - Multiple cavities phase alignment necessary
External (drop configuration)	- Potentially easier to operate singlemode at higher levels of feedback than all-pass external configuration	- Narrower negative optical feedback bandwidth - Lower responsivity of negative optical feedback - Multiple cavities phase alignment necessary
Internal	- Lowest sensitivity to laser operating frequency - Simplest operation - Straightforward single-mode design and operation	- Smaller linewidth improvement - Higher probability of being limited by non-linear effects at high intra-cavity intensities

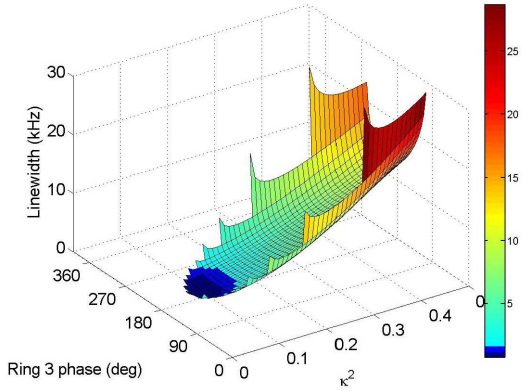

Fig. 23. Instantaneous linewidth as a function of ring 3 phase and coupling strength (ring 3 is aligned with SWF for 180°, propagation loss 0.5 dB/cm).

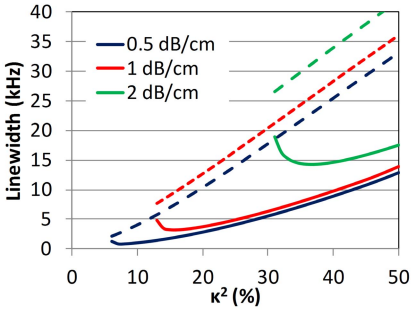

Fig. 24. Instantaneous linewidth as a function of ring 3 coupling strength for various propagation losses. Ring is aligned (180° phase in Fig. 23). (Full lines) Minimum linewidth with detuning, (Dashed lines) linewidth at ring resonance. Linewidth generally improves with reducing the coupling strength (increasing the loaded Q), until the excess loss in cavity (increased insertion loss of ring 3) starts to dominate. The analysis ignores non-linear effects that can limit performance for high-Q values.

We show linewidth only if $R_{eff} > 30\%$. It appears that for lowest linewidth, the Q should be maximized, and that is indeed true until the intra-cavity losses (due to insertion loss of ring, see Fig. 16) or non-linear effects and two-photon absorption start to limit performance. We show the influence of propagation loss of the waveguide platform on linewidth

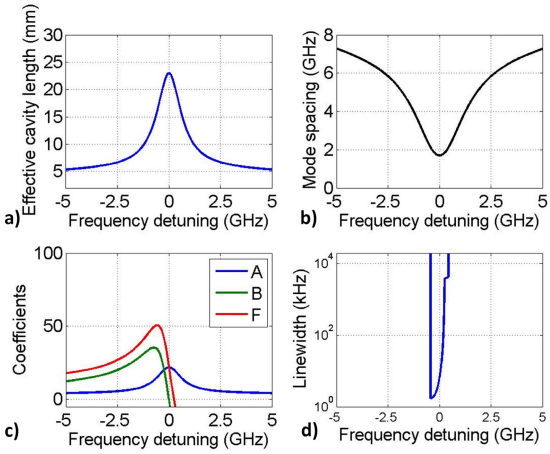

Fig. 25. (a) Effective cavity length (b) Longitudinal mode spacing (c) Coefficients A, B and F (d) Theoretically estimated instantaneous linewidth, all as a function of laser detuning from ring 3 resonance. By slight detuning from the resonance ~1.5 kHz instantaneous linewidth at output power of 3 dBm is obtainable. With higher output powers, sub-kHz instantaneous linewidth should be obtainable. ($\kappa^2 = 15\%$, propagation loss 0.5 dB/cm, ring 3 is aligned to SWF).

in Fig. 24. Nonlinear effects can also be a problem, as they are accentuated inside the resonators due to the intensity enhancement factor [21]. We have considered 3 dBm output powers in our linewidth calculations, which can easily be increased by utilizing booster semiconductor optical amplifiers without increasing the field intensity inside the laser cavity [4].

Finally in Fig. 25 we show, in more detail, the linewidth performance as a function of the detuning of the laser from ring resonance. We show only the case when $\kappa^2 = 15\%$ for ring 3. Compared to the external cavity ring configurations, behavior is more predictable with optimal regions being ~0.5 GHz wide, making the operation of such a laser simplified and more resilient to temperature or other fluctuations.

High-Q ring could also be placed inside the laser cavity in an all-pass configuration, but in such a configuration the high-Q ring does not help with filtering out a single longitudinal mode making single-mode operation very difficult.

V. Conclusion

We have theoretically compared the narrow-linewidth performance of widely-tunable monolithically integrated semiconductor lasers utilizing a high-Q ring resonator (intrinsic $Q \sim 1$ million). The high-Q resonator can be used as an external cavity to provide feedback, or as an integral part of the laser cavity. Each approach has its advantages and disadvantages (summarized in Table I), but considering all of the aspects of the laser design as well as simplicity of operation we conclude that using a high-Q ring as an integral part of the laser cavity is the best approach in order to realize widely-tunable narrow-linewidth monolithically integrated semiconductor lasers. By utilizing heterogeneous integration providing optimized silicon waveguides with low propagation loss, kHz and even sub-kHz instantaneous linewidths should be attainable with proper design. At this level of performance, temperature, vibration and 1/f noise start to dominate, so lasers should be properly isolated and low-noise current sources should be used.

Acknowledgment

Authors would like to thank S. Srinivasan of UCSB and E. Norberg of Aurrion for useful discussions.

References

[1] W. Idler, M. Schilling, G. Laube, K. Wunstel, and O. Hildebrand, "Y laser with 38 nm tuning range," *Electron. Lett.*, vol. 27, no. 24, pp. 2268–2270, Nov. 1991.

[2] V. Jayaraman, Z.-M. Chuang, and L. A. Coldren, "Theory, design, and performance of extended tuning range semiconductor lasers with sampled gratings," *IEEE J. Quantum Electron.*, vol. 29, no. 6, pp. 1824–1834, Jun. 1993.

[3] M. Seimetz, "Laser linewidth limitations for optical systems with high-order modulation employing feed forward digital carrier phase estimation," in *Proc. OFC*, Feb. 2008, pp. 1–3, paper OTuM2.

[4] N. Kobayashi *et al.*, "Silicon photonic hybrid ring-filter external cavity wavelength tunable lasers," *J. Lightw. Technol.*, vol. 33, no. 6, pp. 1241–1246, Mar. 15, 2015.

[5] T. Komljenovic, S. Srinivasan, E. Norberg, M. Davenport, G. Fish, and J. E. Bowers, "Widely tunable narrow-linewidth monolithically integrated external-cavity semiconductor lasers," *IEEE J. Sel. Topics Quantum Electron.*, vol. 21, no. 6, Nov./Dec. 2015, Art. ID 1501909.

[6] M. Larson *et al.*, "Narrow linewidth sampled-grating distributed Bragg reflector laser with enhanced side-mode suppression," in *Opt. Fiber Commun. Conf. OSA Tech. Dig.*, 2015, paper M2D.1.

[7] C. Santis, Y. Vilenchik, A. Yariv, N. Satyan, and G. Rakuljic, "Sub-kHz quantum linewidth semiconductor laser on silicon chip," in *Proc. CLEO*, 2015, paper JTh5A.7.pdf.

[8] B. Liu, A. Shakouri, and J. E. Bowers, "Passive microring-resonator-coupled lasers," *Appl. Phys. Lett.*, vol. 79, no. 22, pp. 3561–3563, 2001. [Online]. Available: http://dx.doi.org/10.1063/1.1420585

[9] B. Liu, A. Shakouri, and J. E. Bowers, "Wide tunable double ring resonator coupled lasers," *IEEE Photon. Technol. Lett.*, vol. 14, no. 5, pp. 600–602, May 2002.

[10] J. C. Hulme, J. K. Doylend, and J. E. Bowers, "Widely tunable Vernier ring laser on hybrid silicon," *Opt. Exp.*, vol. 21, no. 17, pp. 19718–19722, Aug. 2013.

[11] S. Srinivasan, M. Davenport, T. Komljenovic, J. Hulme, D. T. Spencer, and J. E. Bowers, "Coupled-ring-resonator-mirror-based heterogeneous III–V silicon tunable laser," *IEEE Photon. J.*, vol. 7, no. 3, Jun. 2015, Art. ID 2700908.

[12] T. Segawa, S. Matsuo, T. Kakitsuka, T. Sato, Y. Kondo, and R. Takahashi, "Semiconductor double-ring-resonator-coupled tunable laser for wavelength routing," *IEEE J. Quantum Electron.*, vol. 45, no. 7, pp. 892–899, Jul. 2009.

[13] L. A. Coldren, S. W. Corzine, and M. L. Mashanovitch, *Diode Lasers and Photonic Integrated Circuits*, 2nd ed. New York, NY, USA: Wiley, Mar. 2012.

[14] R. F. Kazarinov and C. H. Henry, "The relation of line narrowing and chirp reduction resulting from the coupling of a semiconductor laser to passive resonator," *IEEE J. Quantum Electron.*, vol. 23, no. 9, pp. 1401–1409, Sep. 1987.

[15] D. R. Hjelme, A. R. Mickelson, and R. G. Beausoleil, "Semiconductor laser stabilization by external optical feedback," *IEEE J. Quantum Electron.*, vol. 27, no. 3, pp. 352–372, Mar. 1991.

[16] K. Aoyama, R. Yoshioka, N. Yokota, W. Kobayashi, and H. Yasaka, "Optical negative feedback for linewidth reduction of semiconductor lasers," *IEEE Photon. Technol. Lett.*, vol. 27, no. 4, pp. 340–343, Feb. 15, 2015.

[17] W. Lewoczko-Adamczyk *et al.*, "Ultra-narrow linewidth DFB-laser with optical feedback from a monolithic confocal Fabry–Perot cavity," *Opt. Exp.*, vol. 23, no. 8, pp. 9705–9709, 2015.

[18] H. Yasaka, Y. Yoshikuni, and H. Kawaguchi, "FM noise and spectral linewidth reduction by incoherent optical negative feedback," *IEEE J. Quantum Electron.*, vol. 27, no. 2, pp. 193–204, Feb. 1991.

[19] M. Hossein-Zadeh and K. J. Vahala, "Importance of intrinsic-Q in microring-based optical filters and dispersion-compensation devices," *IEEE Photon. Technol. Lett.*, vol. 19, no. 14, pp. 1045–1047, Jul. 15, 2007.

[20] R. Mancini, *Op Amps For Everyone: Design Reference*. Dallas, TX, USA: Texas Instruments, 2002.

[21] D. G. Rabus, *Integrated Ring Resonators: The Compendium*. New York, NY, USA: Springer-Verlag, 2007.

Tin Komljenovic received the M.Sc. and Ph.D. degrees in electrical engineering from the Faculty of Electrical Engineering and Computing, University of Zagreb, in 2007 and 2012, respectively. During his Ph.D., he was a Visiting Researcher with IETR, University of Rennes. He is currently a Post-Doctoral Researcher with the University of California at Santa Barbara, pursuing research on photonic integration. He has authored or co-authored over 30 papers and holds two patents. His current research interests include optical access networks, wavelength-division multiplexed systems, and tunable optical sources. He received the EuMA Young Scientist Prize for his work on spherical lens antennas and is a recipient of the Marie Curie Fellowship.

John E. Bowers (S'78–M'81–SM'85–F'93) received the M.S. and Ph.D. degrees from Stanford University. He was with AT& Bell Laboratories and Honeywell. He holds the Fred Kavli Chair in Nanotechnology, and is the Director of the Institute for Energy Efficiency and a Professor with the Departments of Electrical and Computer Engineering and Materials, University of California at Santa Barbara. He is the Co-Founder of Aurrion, Aerius Photonics, and Calient Networks. He has authored ten book chapters, 600 journal papers, 900 conference papers, and holds 54 patents. His research is primarily in optoelectronics and photonic integrated circuits. He is a member of the National Academy of Engineering and a fellow of OSA and the American Physical Society. He is a recipient of the OSA/IEEE Tyndall Award, the OSA Holonyak Prize, the IEEE LEOS William Streifer Award, and the South Coast Business and Technology Entrepreneur of the Year Award. He and his co-workers received the EE Times Annual Creativity in Electronics (ACE) Award for Most Promising Technology for the heterogeneous silicon laser in 2007.